proceedings

Proceedings

Spin Rate Measurements in Cricket Bowling Using Magnetometers †

Aswath Kumar, Hugo G. Espinosa *, Matthew Worsey and David V. Thiel

Griffith School of Engineering and Built Environment, Griffith University, Nathan Campus, Brisbane, QLD 4111, Australia; aswathk.1995@gmail.com (A.K.); matthew.worsey@griffithuni.edu.au (M.W.); d.thiel@griffith.edu.au (D.V.T.)

* Correspondence: h.espinosa@griffith.edu.au; Tel.: +61-737-355-084

† Presented at the 13th conference of the International Sports Engineering Association, Online, 22–26 June 2020.

Published: 15 June 2020

Abstract: The ability to measure and classify spin has been of great interest to cricket organizations, coaches, and athletes. While video is common, an alternative approach is to use 3D motion capture analysis with reflective spheres, which changes the aerodynamics of the ball. An instrumented cricket ball has proved to be effective in measuring high-speed spin rates using gyroscopes. In this study, an instrumented ball with a 3-axis accelerometer, 3-axis gyroscope, and 3-axis magnetometer located at the center mass of the ball was constructed. The spin rate was calculated using the magnetometer, and two spin types (off-spin and leg-spin) were classified. The sensor data was validated using motion capture. In addition, inertial measurement units (IMUs) mounted on the wrist and elbow of a wrist-spin and off-spin bowler were used to verify and validate the spin classification. The magnetometer can be effectively used in conjunction with conventional IMU sensors on the bowler's arm to tailor training sessions by addressing deficiencies identified in a bowler's spinning technique and to monitor their performance.

Keywords: cricket; off-spin; leg-spin; inertial sensors; bowling; magnetometer; gyroscope; IMU

1. Introduction

The ability to measure and analyze sporting activities has been of great interest to the cricketing fraternity, including players and coaches, and it has been valued by cricket organizations [1]. The use of wearable inertial sensors has powered the sports technology industry seeking sports performance enhancement [2]. Cricket bowling has been tracked using inertial sensors on the bowler's body to provide feedback [3]. The use of an instrumented cricket ball has also been of interest in implementing a low-cost training analysis tool [4]. This can be used in conjunction with conventional biomechanical analysis to tailor training sessions and to address deficiencies and improvements in a bowler's spinning technique.

A commercially available 9DOF magnetic-inertial sensor (Metawear CPRO from MBientLab Inc., San Francisco, CA, USA [5]) was mounted inside the center of a cricket ball without affecting the seam of the ball. Data from the sensor was used to analyze the bowling characteristics of spin bowlers such as flight time, spin rate, type of spin bowling, and torque force at ball release.

Instrumented cricket balls have been developed for academic and commercial purposes since 2007. Fuss et al. [6] reported a smart cricket ball that incorporates high-speed gyroscopes (±50 rps) for bowling measurements. SportCor (sportcor.com) powered by Kookaburra (kookaburra.biz) currently produces "smart cricket balls" using high-speed inertial sensors inside a protective core, making it resilient under impact [7]. Training data has been modeled into test data using a regression model algorithm to determine motion properties such as spin rate and speed, post-bounce spin rate, and pre-bounce spin rate [7]. Several studies have reported the measurement of spin rate. Spin rates measured by Fuss et al. [6] used gyroscopes with an angular velocity range of ±350 rad/s. The bowling trajectory of a baseball was traced using synchronized high-speed video cameras (250 Hz) and the measurement of spin rates was calculated using markers on the ball (Tsutomu Jinji & Shinji Sakurai [8]).

The kinematics of bowlers using 3D motion analysis of the body included the release characteristics (Chin et al. [9]). High-speed cameras used by Cork et al. (Photron FASTCAM ultima APX high-speed video camera) measured the flight characteristics together with Hawk-Eye ball-tracking software [10]. The kinematic differences between off-spin and leg-spin deliveries using motion analysis were investigated by Beach et al. [11]. They found significant differences in the approach phase, delivery phase, and ball release arm position. The differences between off-spin and doosra (a spin bowling technique) revealed that a significantly larger pelvic rotation is required for an off-spin delivery [12]. Classification algorithm models have also been incorporated by Baker [12] for the prediction of cricket ball trajectories in spin and swing bowling.

Inertial measurement unit (IMU) sensors and 3D motion analysis can be used to identify and quantify different types of bowling actions. This paper reports the spin rate of ball delivery using a magnetometer on an in-house-developed instrumented cricket ball. In addition, multiple IMU sensors on the bowler's arm, as well as the use of infrared-marker camera analysis, were used to identify differences between bowling types.

2. Materials and Methods

2.1. Instrumented Ball

MetaWear CPRO is a 24 mm diameter IMU (Figure 1a) [5], which records acceleration (±16 g), angular velocity (±2000°/s) and magnetic field (±1300 μT *x*-*y* axis, ±2500 μT *z*-axis, and 0.3 μT resolution). The sensor is enclosed in a splash-proof plastic case (Figure 1b). To preserve some of the characteristics of the ball, such as the seam and ball smoothness, the ball was consciously not cut through the seam, instead, the inner core of the ball was cut radially through the center of the side wall using a drill powered lathe. The hole diameter (27.5 mm) was cored on one side of the ball and the sensor was inserted. The sensor was enclosed into a foam-based damping structure. The removed portion was then re-inserted back into the ball and glued with silicone (Figure 1c). Although some of the properties of the ball were slightly affected (i.e., weight and shape), they did not disturb the overall spin rate analysis. A preliminary development of the instrumented ball can be found in reference [13].

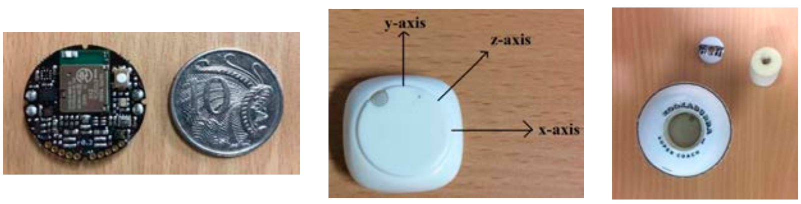

(**a**) (**b**) (**c**)

Figure 1. (**a**) MetaWear CPRO (mbientlab.com); (**b**) axes orientation on the MetaWear CPRO sensor placed inside a plastic case; (**c**) insertion of the sensor into the side of an indoor cricket ball.

2.2. IMU and Motion Capture

Three identical 9DOF IMU sensors (Sabel Sense, Griffith University, Griffith, Australia [14]) each with 250 Hz sampling rate, ±16 g accelerometer, ±2000°/s gyroscope, ±7 Gauss magnetometer, and a weight of 23 g, were attached to the participant's lumbar upper back (T3) and wrist (Figure 2). Retro-reflective markers were positioned on the bowler's body for motion capture analysis. The use of IMU sensors along with the 3D markers assessed the correlation of the marker positions with the acceleration data.

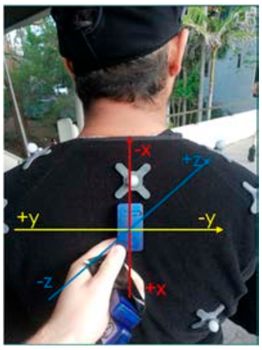

Figure 2. Retro-reflective markers and inertial measurement unit (IMU) sensors on the bowler's body.

2.3. Sensor Calibration

A computer-controlled motor was used to measure the spin rate accuracy (Figure 3). A 3D printed "chuck" was designed to hold the ball centrally. A stepper motor was mounted on a wooden base and tightened. The microcontroller (Arduino-Uno, Arduino LLC, New York, NY, USA) was used to set the rotation speed. This standard rotation model was then used to calibrate the spin rate measured on the magnetometer. The standard value of the difference between spin rate defined by the user and measured by the magnetometer was considered as a calibration factor for spin rate measurements.

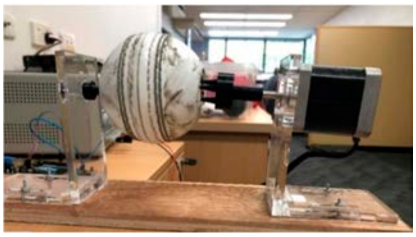

Figure 3. Microcontroller calibration setup.

3. Results

3.1. Spin Rate Measurement

The accelerometer, gyroscope, and magnetometer data from the ball were recorded in the target period for spin rate analysis. Figure 4a shows the peak acceleration during ball release and pitch (top), and the angular velocity change on the gyroscope (middle). Magnetometer readings show a significant rise and fall when the ball was manually rotated in the air and following a bounce (Figure 4b).

The spin rate f was calculated from the magnetometer readings as

$$f = \frac{1}{\sum(T_{i+1} - T_i)} \tag{1}$$

where T is the mean of the time difference between each ith rotation peak. The pre-bounce and post-bounce spin rates were determined from the impact point of the accelerometer at the time of release, and at the first point of the pitch. The ratio of the post-bounce spin rate and pre-bounce spin rate shows the significant spin produced from the pitch. The peak points of the samples were in time T, and the mean time between peaks was calculated for pre-bounce and post-bounce, which is indicated in Figure 4b with blue and red peak circles.

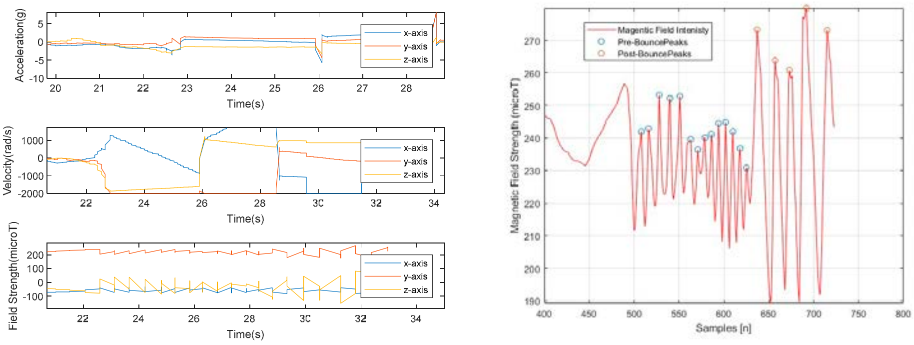

(**a**) (**b**)

Figure 4. (**a**) IMU sensor readings of a spinning ball (acceleration—top, gyroscope—middle and magnetometer—bottom); (**b**) pre-bounce and post-bounce peaks of a spinning ball for the magnetometer.

3.2. Characteristics of the Spin Bowler

The angular velocity of the ball was calculated from the gyroscope and the average torque was analyzed using the peak acceleration. The peak time was calculated from the acceleration plot. This is indicated with red dots in Figure 5, which shows the flight time between two peak points (point of release and pitching).

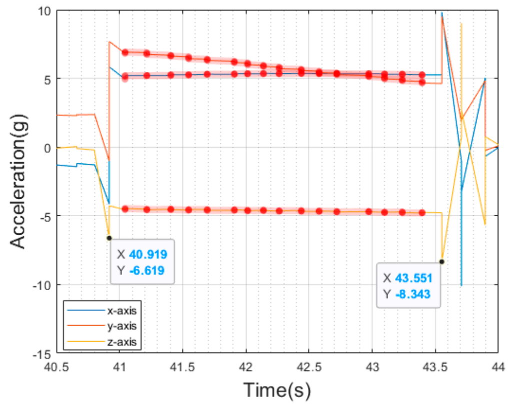

Figure 5. Flight time measurements of a spinning ball.

3.3. Spin Type Classification

Initial tests for off-spin and leg-spin showed consistent differences in the spin rate observed from the magnetometer reading. The time-domain signals of the leg-spin and of the off-spin bowlers were converted to the frequency domain using a Fourier transform in order to calculate the average central frequency. The central frequency is higher for leg-spin (Figure 6a) than for off-spin (Figure 6b) as shown in Table 1. This clearly shows a higher spin rate for wrist spinners.

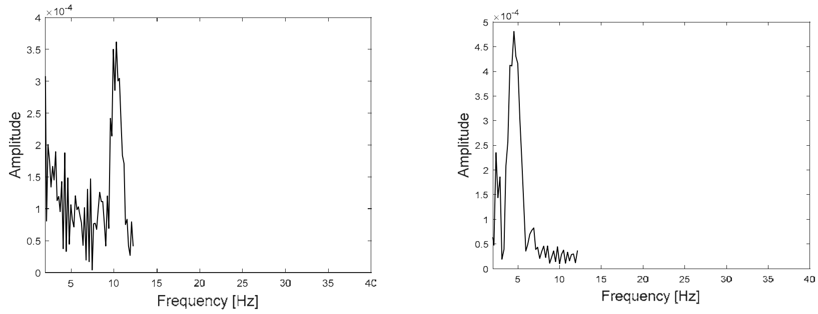

(**a**) (**b**)

Figure 6. (**a**) Frequency domain for leg-spin balls; (**b**) frequency domain for off-spin balls.

Table 1. Comparison between off-spin and leg-spin in the frequency domain.

Type of Spin	Average Peak Central Frequency (Hz)	Average Frequency Range (Hz)
Off-spin	7.22	05–10
Leg-spin	11.31	10–13

3.4. Biomechanical Analysis

The biomechanics of the bowler were analyzed primarily using data collected from IMU sensors and retro-reflective markers on the bowler's lumbar T3 (see Figure 2). A regression linear model for classification was used to separate off-spin and leg-spin. Figure 7a shows an "over" of six "deliveries" from a single bowler using motion capture. Magnetic-inertial sensors were also used as a linear model for classification between off-spin and leg-spin bowlers. Figure 7b shows the raw acceleration data from two deliveries.

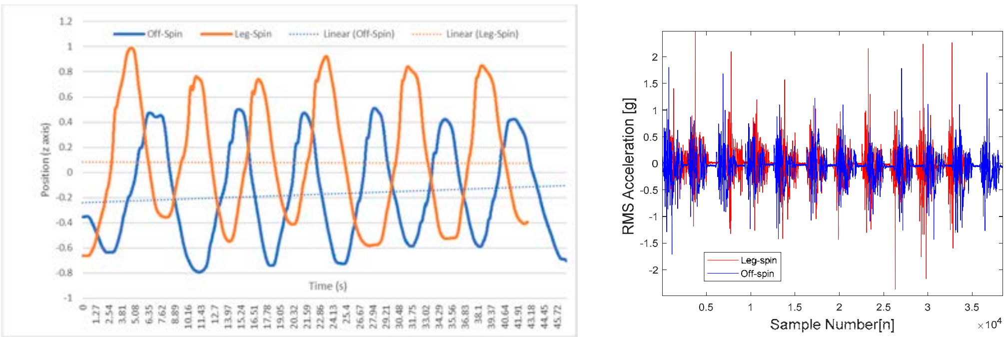

(**a**) (**b**)

Figure 7. Linear classification model for off-spin and leg-spin bowlers: (**a**) motion capture; (**b**) root mean square (RMS) acceleration of the bower's lumbar (T3) using IMU sensors sampled at 250 Hz.

Several superimposed bowls with an IMU located on the bowler's wrist are shown in Figure 8. The red line in both plots indicates the average root mean square (RMS) acceleration of all bowls. A higher acceleration (7.5 g) can be observed in leg-spin bowls (Figure 8a) when compared to the acceleration (5 g) of the off-spin bowls (Figure 8b).

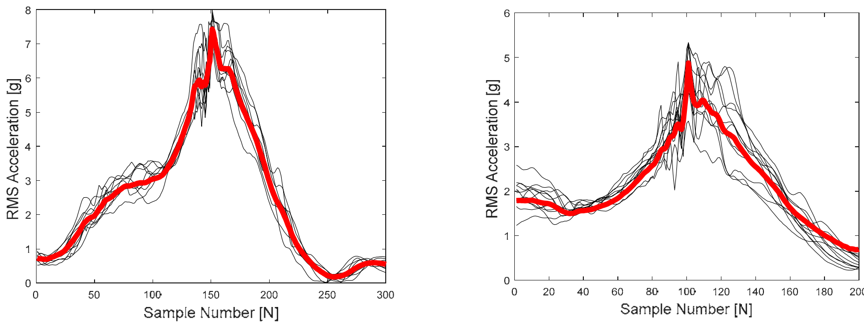

(**a**) (**b**)

Figure 8. RMS acceleration of the wrist using IMU sensors sampled at 250 Hz: (**a**) accelerometer readings of off-spin balls; (**b**) accelerometer readings of leg-spin balls.

4. Discussion

The spin parameters and bowler motion included spin rate, flight time, torque at point of release, angular velocity, and acceleration at release point. The flight time measurement (red dots in Figure 5) was similar to the results obtained by Fuss et al. [6]—dropping from 17.5 rps to 16.33 rps within 2 s flight time. Leg-spin release was found to have a higher spin rate than off-spin. While only low spin rates were possible using the magnetometer due to lower sampling frequency, it was still observed that wrist spinners have a higher average spin rate (10 rps) compared to off spinners (7 rps). This 30%

difference is close to the results obtained by Beach et al. [11]. Ground reaction forces at the point of release can also be marked as an important location on the bowler's body for recognizing the bowler's action [3]. Future work focuses on machine learning models to be tested on experimental data to evaluate the plausibility of classifying bowling types using an instrumented cricket ball and IMU sensors attached to key parts of the bowler's body. As every bowler is characterized by a different bowling action, it is important to enhance the preliminary model used in this study with non-linear-based regression models.

5. Conclusions

This paper describes the development of an IMU sensor-instrumented cricket ball that did not significantly alter the ball properties. Measurements of low spin rate bowling were verified using magnetometers. These results are comparable to the spin rates obtained in the literature using gyroscopes. The low-speed limitation can be resolved by using a high-sample-rate-based magnetometer. The ability to record bowling characteristics such as flight time and torque can be used as parameters for addressing the overall bowling training protocols in cricket. The biomechanical properties of the bowler were also found to complement the bowling analysis obtained from the instrumented ball.

Conflicts of Interest: The authors declare no conflict of interest.

References

1. Mehta, R.D. An overview of cricket ball swing. *Sports Eng.* **2005**, *8*, 181–192.
2. Espinosa, H.G.; Shepherd, J.B.; Thiel, D.V.; Worsey, M.T.O. Anytime, anywhere! Inertial sensors monitor sports performance. *IEEE Potentials* **2019**, *38*, 11–16.
3. Rowlands, D.; James, D.A.; Thiel, D.V. Bowler analysis in cricket using centre of mass inertial monitoring. *Sports Technol.* **2009**, *2*, 39–42.
4. Doljin, B.; Fuss, F.K. Development of a smart cricket ball for advanced performance analysis of bowling. *Procedia Technol.* **2015**, *20*, 133–137.
5. MbientLab–Wearable Bluetooth 9-axis IMUs & environmental Sensors. Available online: https://mbientlab.com/ (accessed on 2 October 2019).
6. Fuss, F.K.; Smith, R.M.; Subic, A. Determination of spin rate and axes with an instrumented cricket ball. *Procedia Eng.* **2012**, *34*, 128–133.
7. Tattersfield, B. Smart Ball, Locator System and Method Therefor. U.S. Patent US20190168081A1, 6 June 2019.
8. Jinji, T.; Sakurai, S. Direction of spin axis and spin rate of the pitched baseball. *Sports Biomech.* **2006**, *5*, 197–214.
9. Chin, A.; Elliott, B.; Alderson, B.; Lloyd, D.; Foster, D. The off-break and "doosra": Kinematic variations of elite and sub-elite bowlers in creating ball spin in cricket bowling. *Sports Biomech.* **2009**, *8*, 187–198.
10. Cork, A.; Justham, L.; West, A. Three-dimensional vision analysis to measure the release characteristics of elite bowlers in cricket. *Proc. Inst. Mech. Eng. Part P J. Sports Eng. Tech.* **2013**, *227*, 116–127.
11. Beach, A.J.; Ferdinands, R.E.D.; Sinclair, P.J. The kinematic differences between off-spin and leg-spin bowling in cricket. *Sports Biomech.* **2016**, *15*, 295–313.
12. Baker, C. A unified framework for the prediction of cricket ball trajectories in spin and swing bowling. *Proc. Inst. Mech. Eng. Part P J. Sports Eng. Tech.* **2013**, *227*, 31–38.
13. Espinosa, H.G.; Öchsner, A.; Mirnajafizadeh, A.; James, D.A. On the preliminary design of an instrumented ball for sports applications. *Hum. Technol.* **2016**, *1*, 5–6.
14. Espinosa, H.G.; Lee, J.; James, D.A. The inertial sensor: A base platform for wider adoption in sports science applications. *J. Fitness Res.* **2015**, *4*, 1–8.

© 2020 by the authors. Licensee MDPI, Basel, Switzerland. This article is an open access article distributed under the terms and conditions of the Creative Commons Attribution (CC BY) license (http://creativecommons.org/licenses/by/4.0/).